Double-ϕ production in $\bar{p}p$ reactions near threshold and Scattering length in $\pi^- p \to \phi n$ reaction

Dayoung Lee
Department of Physics, Pukyoung National University (PKNU)
Center for Extreme Nuclear Matters (CENuM), Korea University

Double-ϕ production in $\bar{p}p$ reactions near threshold

I. Introduction

- $\bar{p}p \to \phi\phi$ process is disconnected quark lines, According to the Okubo-Zweing-Iizuka(OZI) rule, this process should be strongly suppressed.

- Data from the JETSET experiment showed a significant violation of the OZI rule.

- Reaction $\bar{p}p \to \phi\phi$ may occur through a two-separate process involving meson pairs, such as $\omega\omega$. Upper limit is $10\mathrm{nb}$ (<experimental data).

- Strange quarks could be knocked off directly from the $\bar{q}q$ sea of the proton and the antiproton. Upper limit is $250\mathrm{nb}$ (<experimental data).

- OZI violation can occur if a resonant glueball like X(2370), which is suspected to be a glueball.

- The $\bar{p}p \to \phi\phi$ reactions can be described in terms of the meson pole and baryon exchange diagrams.

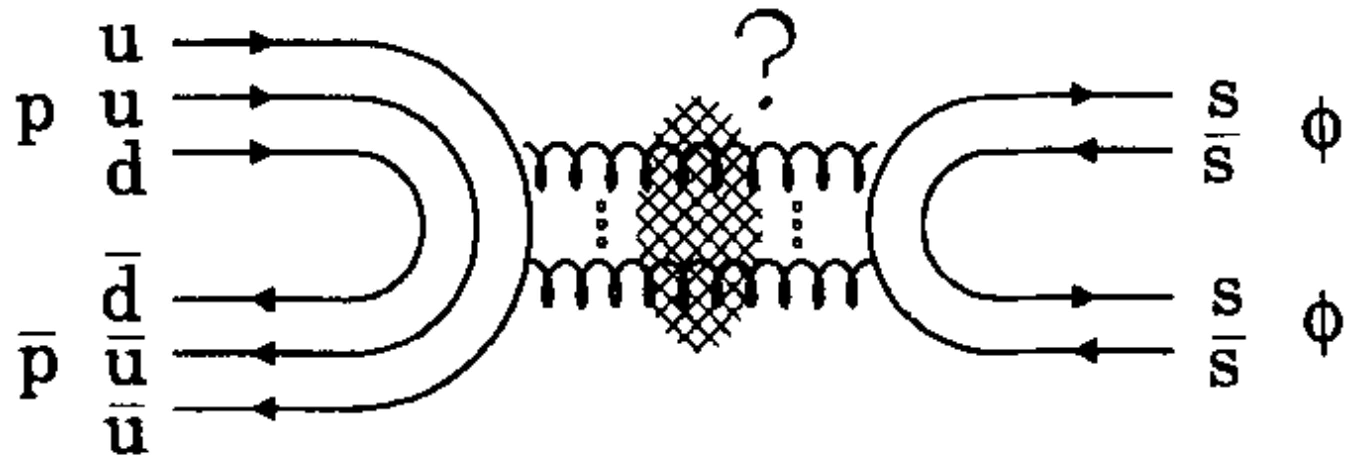

JETSET, Il Nouvo Cimento **107**, 2329 (1994)

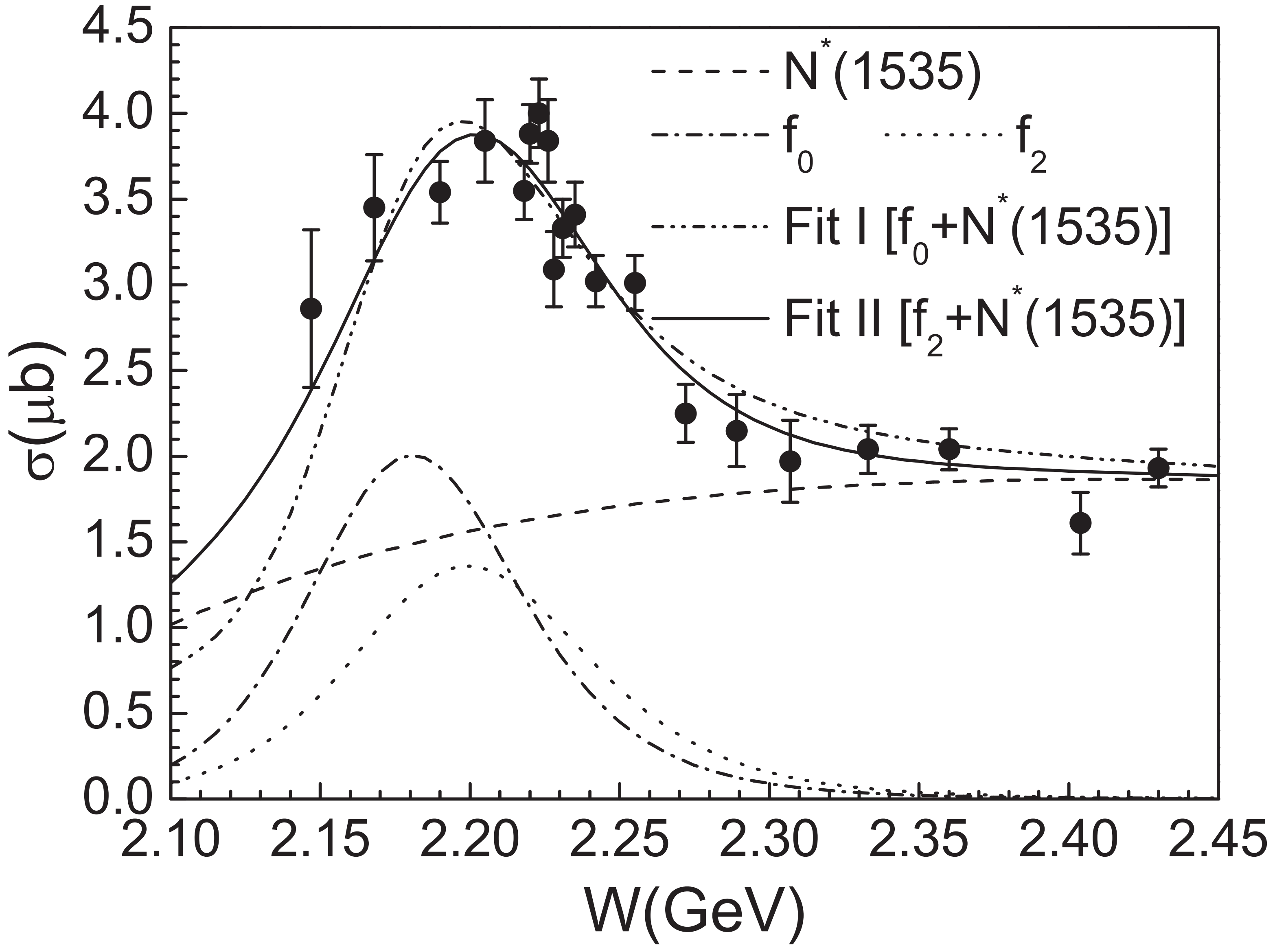

J. J. Xie *et al*, Phys. Rev. C **90**, 048201 (2014)

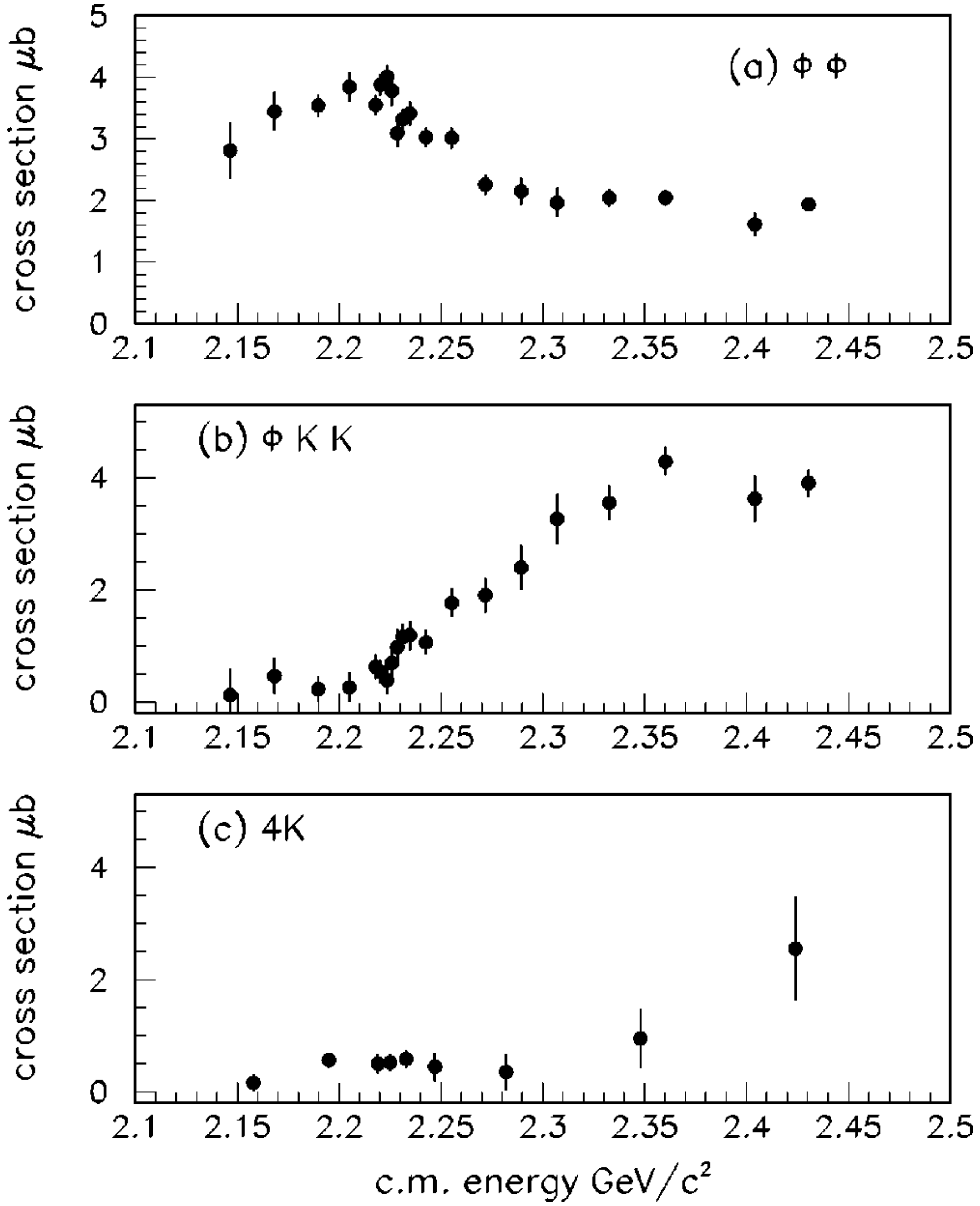

JETSET, Phys. Rev. D **57**, 5370 (1998)

II. Theoretical framework

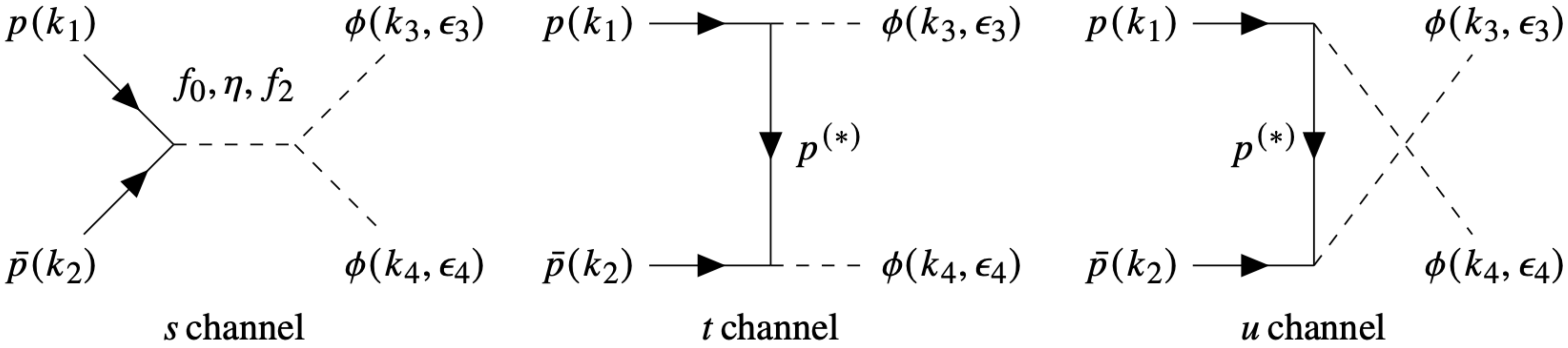

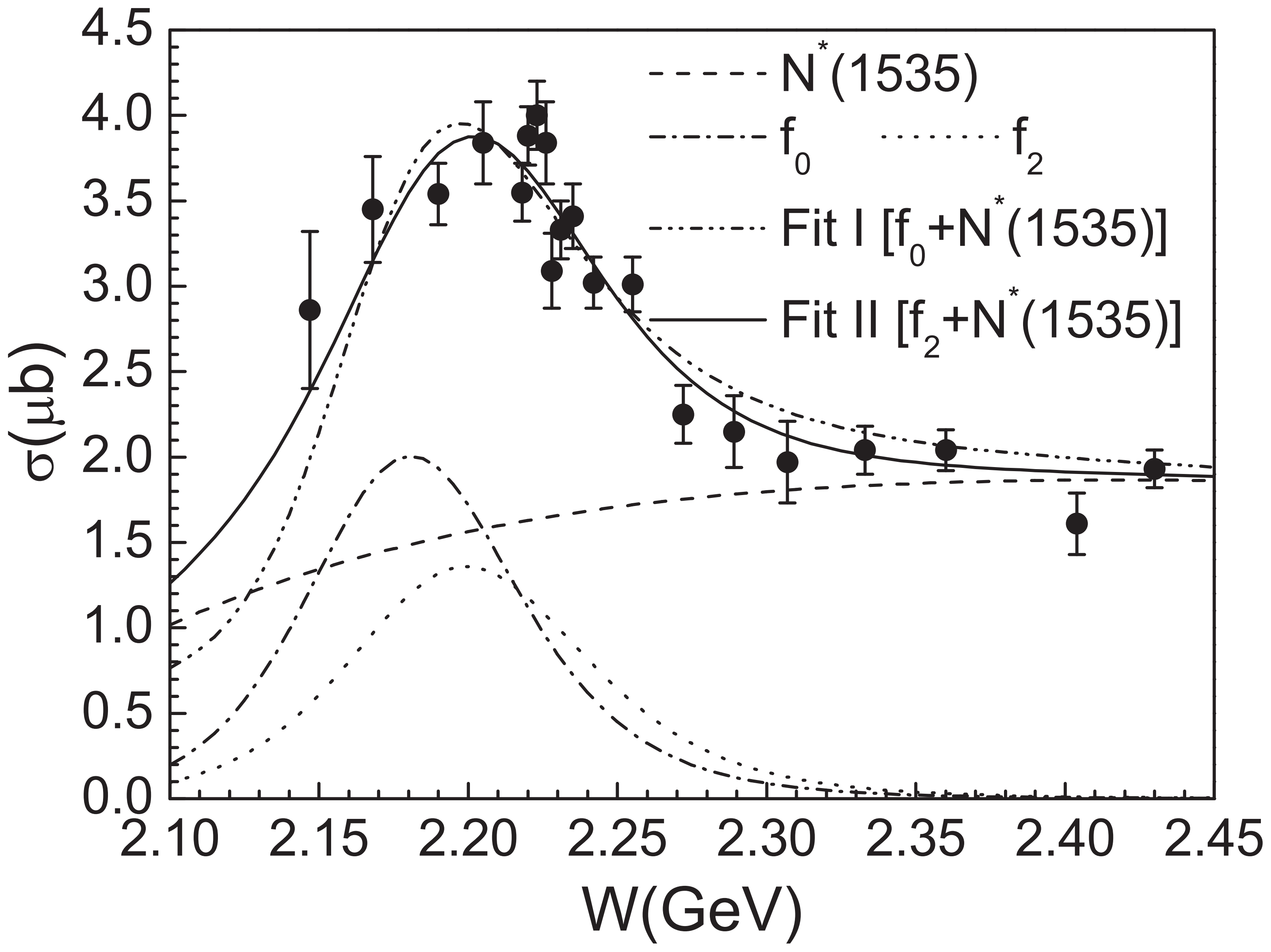

J. J. Xie *et al*, Phys. Rev. C **90**, 048201 (2014)

$f_0(2020, 2100, 2200)$

$f_2(1950, 2010, 2150)$, $\eta(2225)$

$N, N^*(1535, 1/2^-), N^*(1650, 1/2^-),$

$N^*(1895, 1/2^-), P_s(2071, 3/2^-)$

Effective Lagrangians for the interaction of Yukawa vertices

$$\mathcal{L}_{SNN} = g_{SNN}\bar{N}SN + \text{h.c.}, \quad \mathcal{L}_{SVV} = \frac{g_{S\phi\phi}}{m_\phi}\boxed{F_{\mu\nu}F^{\mu\nu}}S \longrightarrow F_{\mu\nu} = \partial_\mu V_\nu - \partial_\nu V_\mu, \text{ self gauge-invariant}$$

$$\mathcal{L}_{PNN} = \frac{f_{PNN}}{M_P}\bar{N}\gamma_5(\partial\!\!\!/ P)N, \quad \mathcal{L}_{PVV} = \frac{ig_{PVV}}{M_P}\epsilon_{\mu\nu\rho\sigma}F_V^{\mu\nu}F_V^{\rho\sigma}P,$$

$$\mathcal{L}_{TNN} = -\frac{ig_{TNN}}{M_N}\bar{N}(\gamma_\mu\partial_\nu + \gamma_\nu\partial_\mu)NT^{\mu\nu} + \text{h.c.}, \quad \mathcal{L}_{TVV} = \frac{g_{TVV}}{2M_V}\left[\frac{g_{\mu\nu}}{4}F_{\rho\sigma}F^{\rho\sigma} - g^{\sigma\rho}F_{\nu\rho}F_{\sigma\mu}\right]T^{\mu\nu},$$

$$\mathcal{L}_{VNN} = -g_{VNN}\bar{N}\gamma_\mu\Gamma_5 NV^\mu, \quad \mathcal{L}_{VNN'} = -\frac{ig_{VNN'}}{M_V}\bar{N}'^{\mu}\gamma^\nu(\partial_\mu V_\nu - \partial_\nu V_\mu)\Gamma_5\gamma_5 N + \text{h.c.},$$

II. Theoretical framework - Hidden-local symmetry and Ward-Takahashi(WT) identity

- When considering the hidden-local symmetry for the ϕ meson, it is essential to uphold the (extended) Ward-Takahashi (WT) identity for the total amplitude.

$$i\mathcal{M}^{\text{total}}_{\mu\nu} k_3^{\mu} = i\mathcal{M}^{\text{total}}_{\mu\nu} k_4^{\nu} = 0$$

$$i\mathcal{M}_S^s = -\frac{2ig_{SVV}g_{SNN}}{M_V} \frac{\bar{\nu}_{k_2}\left[(k_3 \cdot k_4)(\epsilon_3 \cdot \epsilon_4) - (k_3 \cdot \epsilon_4)(\epsilon_3 \cdot k_4)\right] u}{s - M_S^2 + i\Gamma_S M_S} \times F_s^S$$

- Common form factor $F_c^N(t, u)$ is used to satisfy the WT identity in both the t and u channel amplitudes, resulting in $i\mathscr{M}^u_{N,N*} + i\mathscr{M}^t_{N,N*} = 0$ for $\epsilon_{3,4} \to k_{3,4}$.

$$F_x^h \equiv F(x, M_h, \Lambda_h) = \frac{\Lambda_h^4}{\Lambda_h^4 + (x - M_h^2)^2}$$

$$F_c^{N,N^*,N'^*} = 1 - \left(1 - F_t^{N,N^*,N'^*}\right)\left(1 - F_u^{N,N^*,N'^*}\right)$$

$$i\mathcal{M}^{\text{total}}_{\mu\nu} k_3^{\mu} = \left[i\mathcal{M}^s_{f_0\mu\nu} + i\mathcal{M}^s_{f_2\mu\nu} + \sum_{x=t,u} i\mathcal{M}^x_{N\mu\nu} + \sum_{x=t,u} i\mathcal{M}^x_{N^*\mu\nu}\right] k_3^{\mu} = 0$$

II. Theoretical framework - $\bar{\Lambda}\Lambda$ channel opening

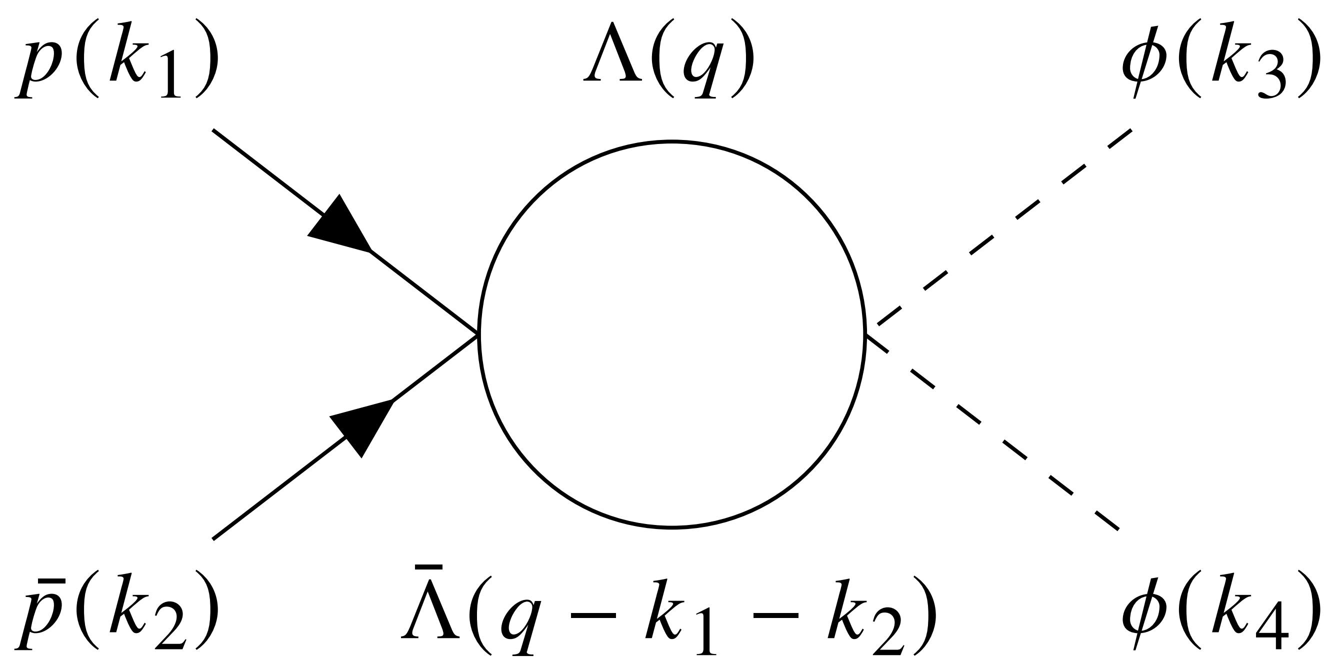

- In $\bar{p}p$ scattering, other $\bar{B}B$ channels can open.
- In the energy region form $W = E_{\text{threshold}}$ to 2.5GeV, $\bar{\Lambda}\Lambda$ channel opening can appear at $W = 2M_\Lambda = 2.232\text{GeV}$.

$$\mathcal{L}_{4B} = \frac{g_{4B}}{M_N^2}\bar{B}B\bar{B}'B', \quad \mathcal{L}_{VBVB} = \frac{g_{VBVB}}{M_N^3}\bar{B}F_{\mu\nu}F^{\mu\nu}B.$$

$$i\mathcal{M}_{\bar{\Lambda}\Lambda} = -g_{\bar{\Lambda}\Lambda}\bar{\nu}\left[(k_3\cdot k_4)(\epsilon_3\cdot\epsilon_4) - (k_3\cdot\epsilon_4)(\epsilon_3\cdot k_4)\right]uF_{\text{loop}}$$

$$\times \underbrace{\int \frac{d^4p}{(2\pi)^4}\frac{\text{Tr}[(\not{p}+M_\Lambda)(\not{p}+\not{q}_{1+2}+M_\Lambda)]}{[p^2-M_\Lambda^2][(p+q_{1+2})^2-M_\Lambda^2]}}_{G_{\bar{\Lambda}\Lambda}(s)},$$

$$G_{\bar{\Lambda}\Lambda}(s) = 4i\int_0^1 dx\left[I^{(2)}_{\bar{\Lambda}\Lambda} - \Delta I^{(0)}_{\bar{\Lambda}\Lambda}\right] = -\frac{i}{4\pi^2}\int_0^1 dx\,\Delta\ln\frac{\Delta_\mu}{\Delta},$$

$$I^{(0)}_{\bar{\Lambda}\Lambda}(x) = \frac{1}{16\pi^2}\ln\frac{\Delta_\mu}{\Delta}, \quad I^{(2)}_{\bar{\Lambda}\Lambda}(x) = -\frac{\Delta}{8\pi^2}\ln\frac{\Delta_\mu}{\Delta}.$$

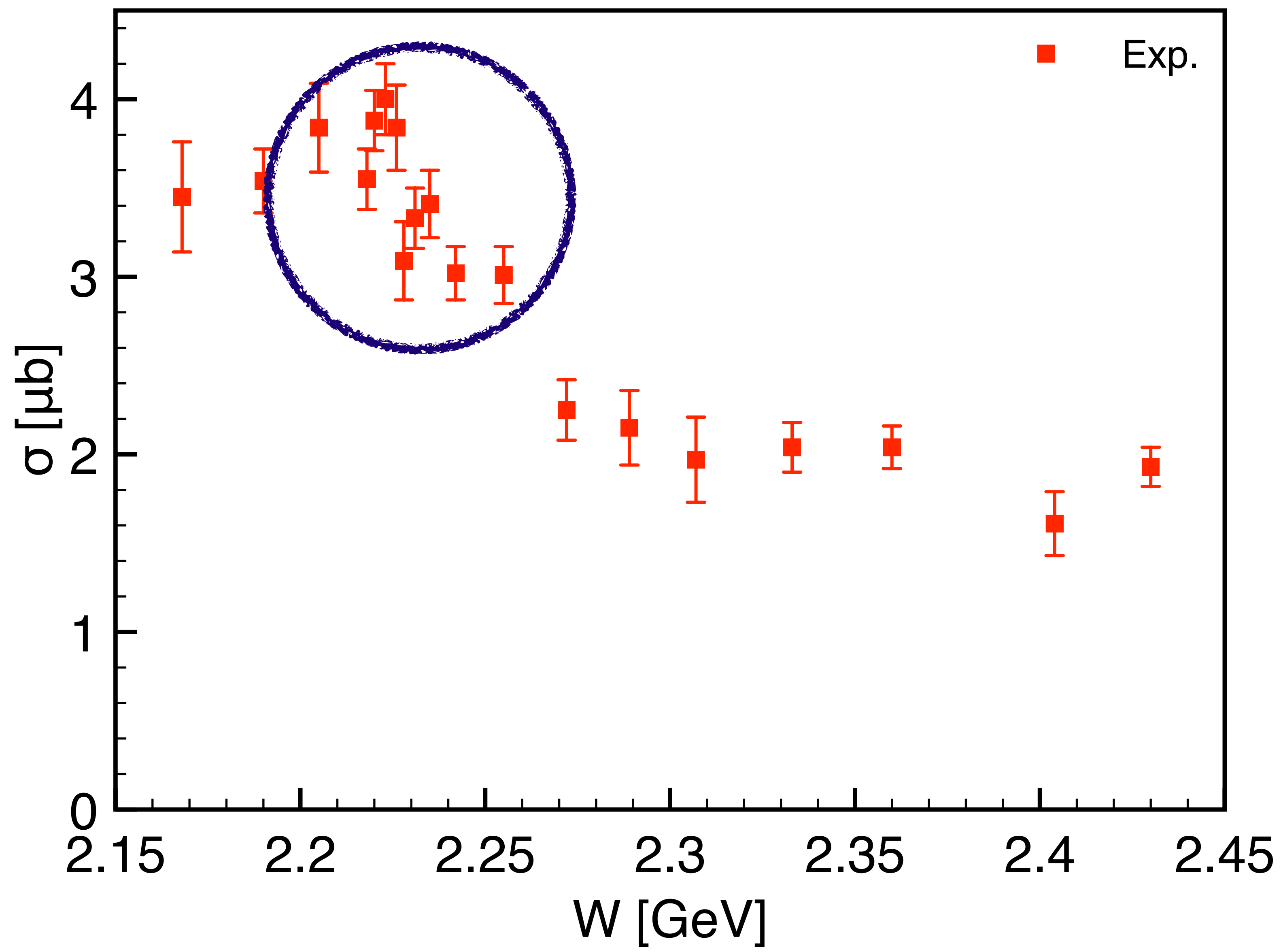

JETSET, Phys. Rev. D **57**, 5370 (1998)

II. Theoretical framework - Spin-Density Matrix Element (SDME)

$$\rho^0_{\lambda_{\phi_3}\lambda'_{\phi_3}} = \frac{1}{2N_T}\sum_{\lambda_p}\sum_{\lambda_{\bar p}}\sum_{\lambda_{\phi_4}=\pm 1}\mathcal{M}_{\lambda_p\lambda_{\bar p}\lambda_{\phi_3}\lambda_{\phi_4}}\mathcal{M}^*_{\lambda_p\lambda_{\bar p}\lambda'_{\phi_3}\lambda_{\phi_4}},\quad N_T = \frac{1}{2}\sum_{\lambda_p}\sum_{\lambda_{\bar p}}\sum_{\lambda_{\phi_3}}\sum_{\lambda_{\phi_4}=\pm 1}|\mathcal{M}_{\lambda_p\lambda_{\bar p}\lambda_{\phi_3}\lambda_{\phi_4}}|^2,$$

$$\rho^4_{\lambda_{\phi_3}\lambda'_{\phi_3}} = \frac{1}{N_L}\sum_{\lambda_p}\sum_{\lambda_{\bar p}}\mathcal{M}_{\lambda_p\lambda_{\bar p}\lambda_{\phi_3}0}\mathcal{M}^*_{\lambda_p\lambda_{\bar p}\lambda'_{\phi_3}0},\quad N_L = \sum_{\lambda_p}\sum_{\lambda_{\bar p}}\sum_{\lambda_{\phi_3}}|\mathcal{M}_{\lambda_p\lambda_{\bar p}\lambda_{\phi_3}0}|^2,$$

- The spin-density matrix element is one of the useful observables in interpreting the reaction mechanism.
- There are nine independent SDMEs, considering the two ϕ-meson helicities.

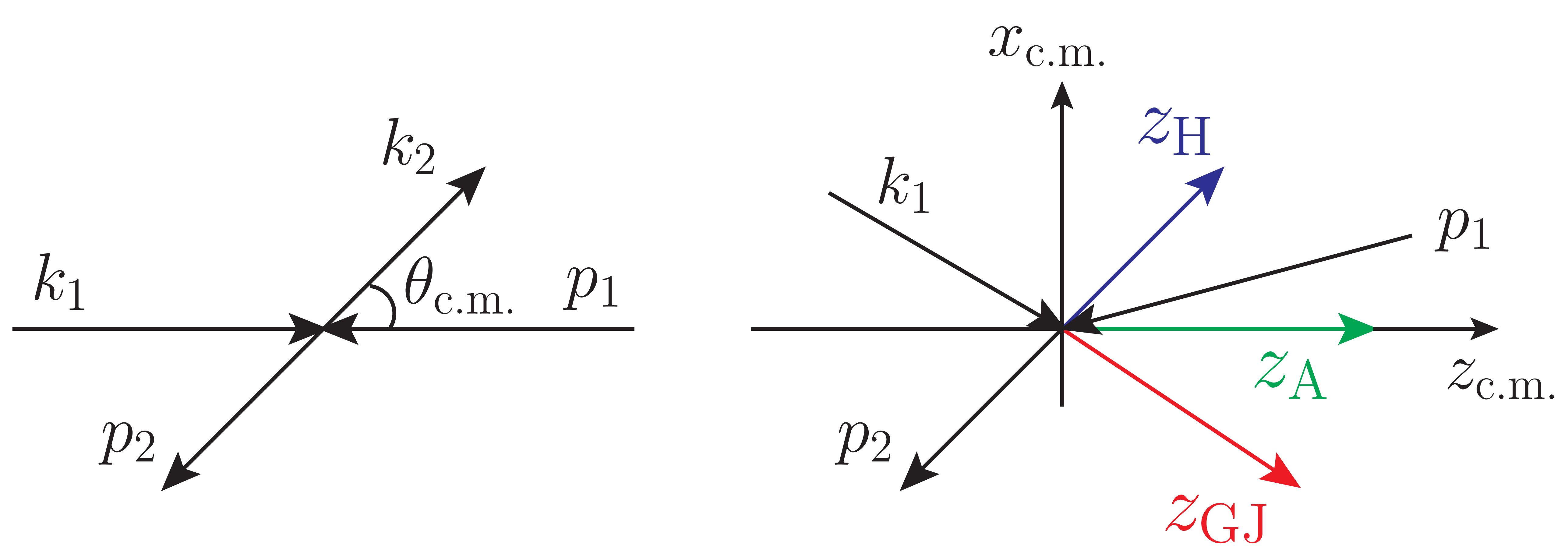

$$d^1(\alpha) = \begin{pmatrix} \frac{1}{2}(1+\cos\alpha) & -\frac{1}{\sqrt{2}}\sin\alpha & \frac{1}{2}(1-\cos\alpha) \\ \frac{1}{\sqrt{2}}\sin\alpha & \cos\alpha & -\frac{1}{\sqrt{2}}\sin\alpha \\ \frac{1}{2}(1-\cos\alpha) & \frac{1}{\sqrt{2}}\sin\alpha & \frac{1}{2}(1+\cos\alpha) \end{pmatrix}$$

$$\rho^B = d^1(-\alpha_{A\to B})\rho^A d^1(\alpha_{A\to B})$$

S. H. Kim *et al*, Phys. Rev. C **100**, 065208 (2019)

III. Numerical results - Total Cross Section

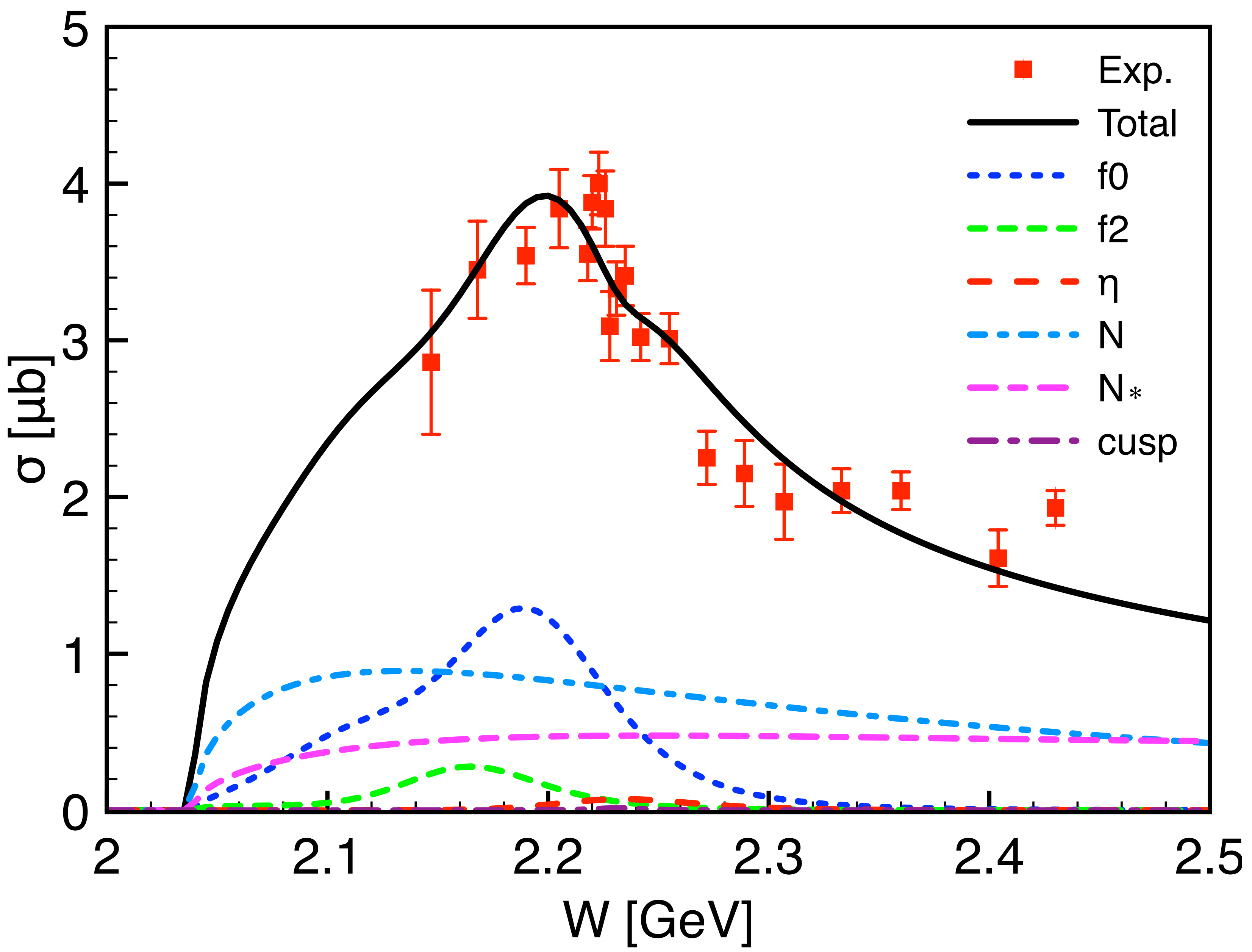

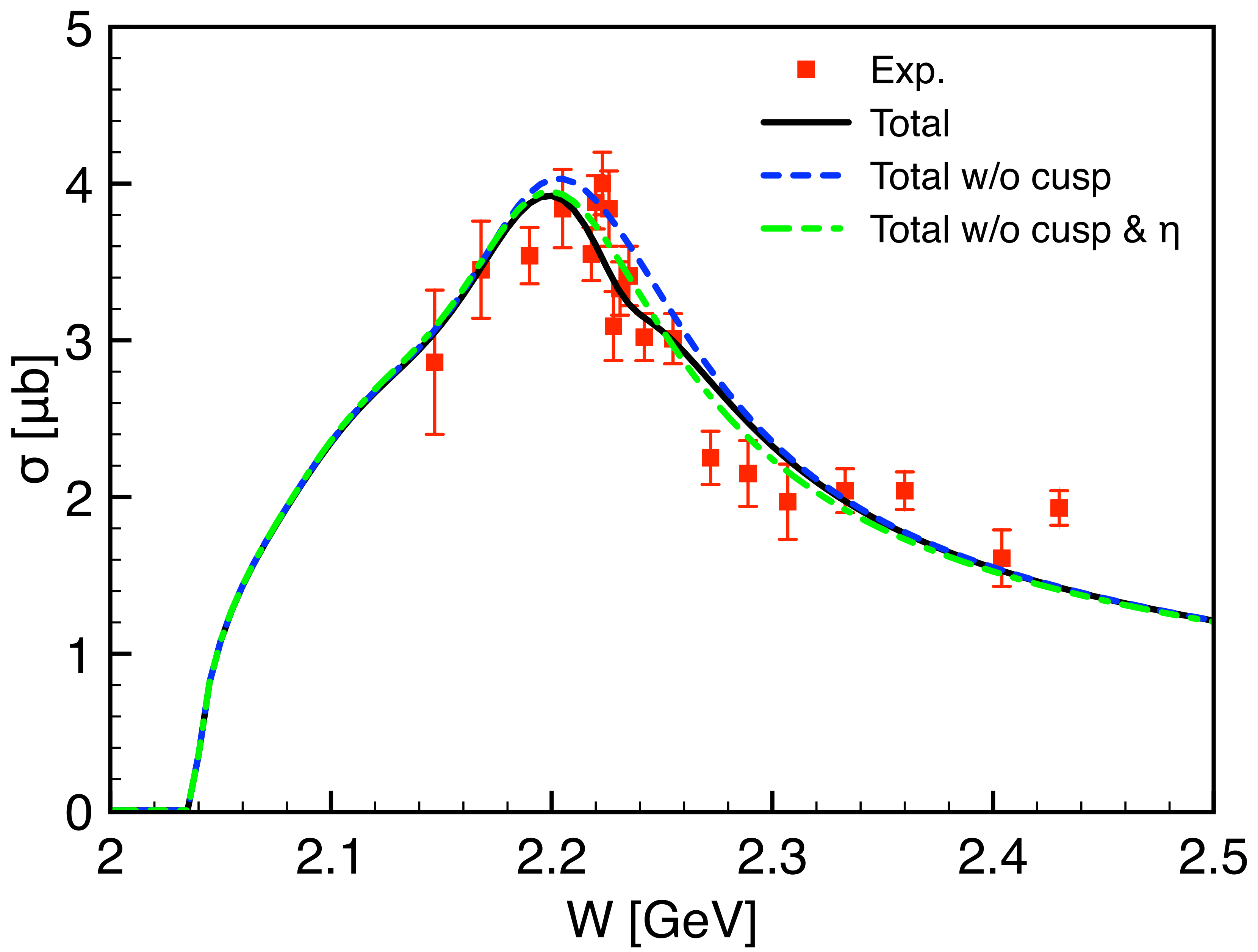

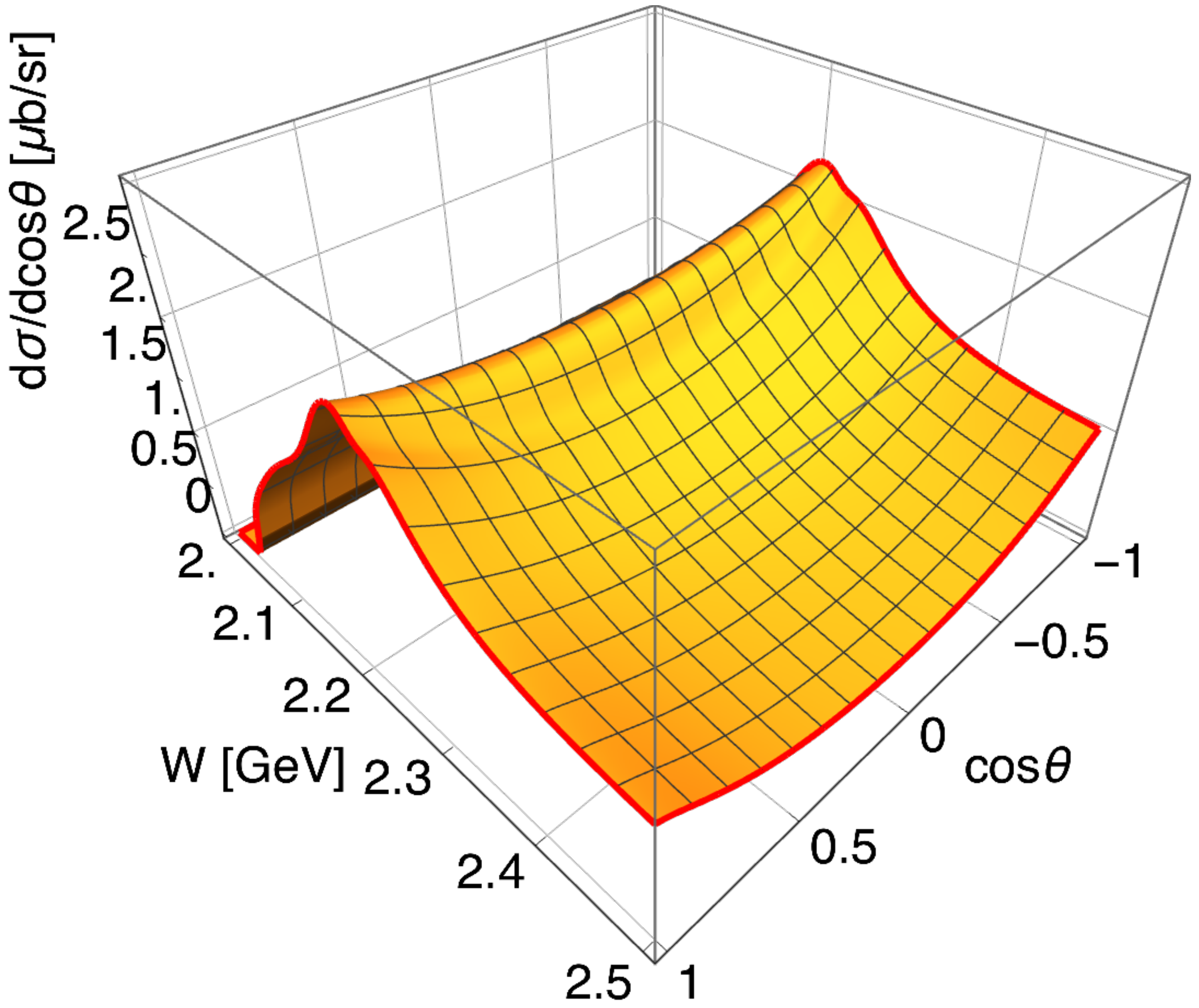

Coupling constants

	$f_0(2020)$	$f_0(2100)$	$f_0(2200)$	$f_2(1950)$	$f_2(2010)$	$f_2(2150)$
$M - i\Gamma/2$ [MeV]	$1982 - i218$	$2095 - i143.5$	$2187 - i103.5$	$1936 - i232$	$2011 - i101$	$2157 - i76$
$g_{(S,P,T)}$	0.115			-0.1		

$$g_{\eta(\phi\phi,NN)} = (-4.062, 0.5)$$

	N	$N^*(1535, 1/2^-)$	$N^*(1650, 1/2^-)$		$N^*(1895, 1/2^-)$		$P_s(2071, 3/2^-)$
$M - i\Gamma/2$ [MeV]	$938 - i0$	$1504 - i55$	$1668 - i28$	$1673 - i67$	$1801 - i96$	$1912 - i54$	$2071 - i7$
$g_{\phi NN^{(*)}}$	-1.47	$1.4 + i2.2$	$4.1 - i2.7$	$4.5 + i5.2$	$2.1 + i1.8$	$0.9 - i0.2$	$0.14 + i0.2$

R. L. Workman *et al*, [Particle Data Group], PTEP **2022**, 083C01 (2022)

K. P. Khemchandani et al, Phys. Rev. D **88**, no.11, 114016 (2013)

III. Numerical results - Total Cross Section

- Total cross section cannot distinguish whether it includes both $N + N^*$ or N^* only.
- We will further discuss the two cases in detail later.

III. Numerical results - Differential Cross Section

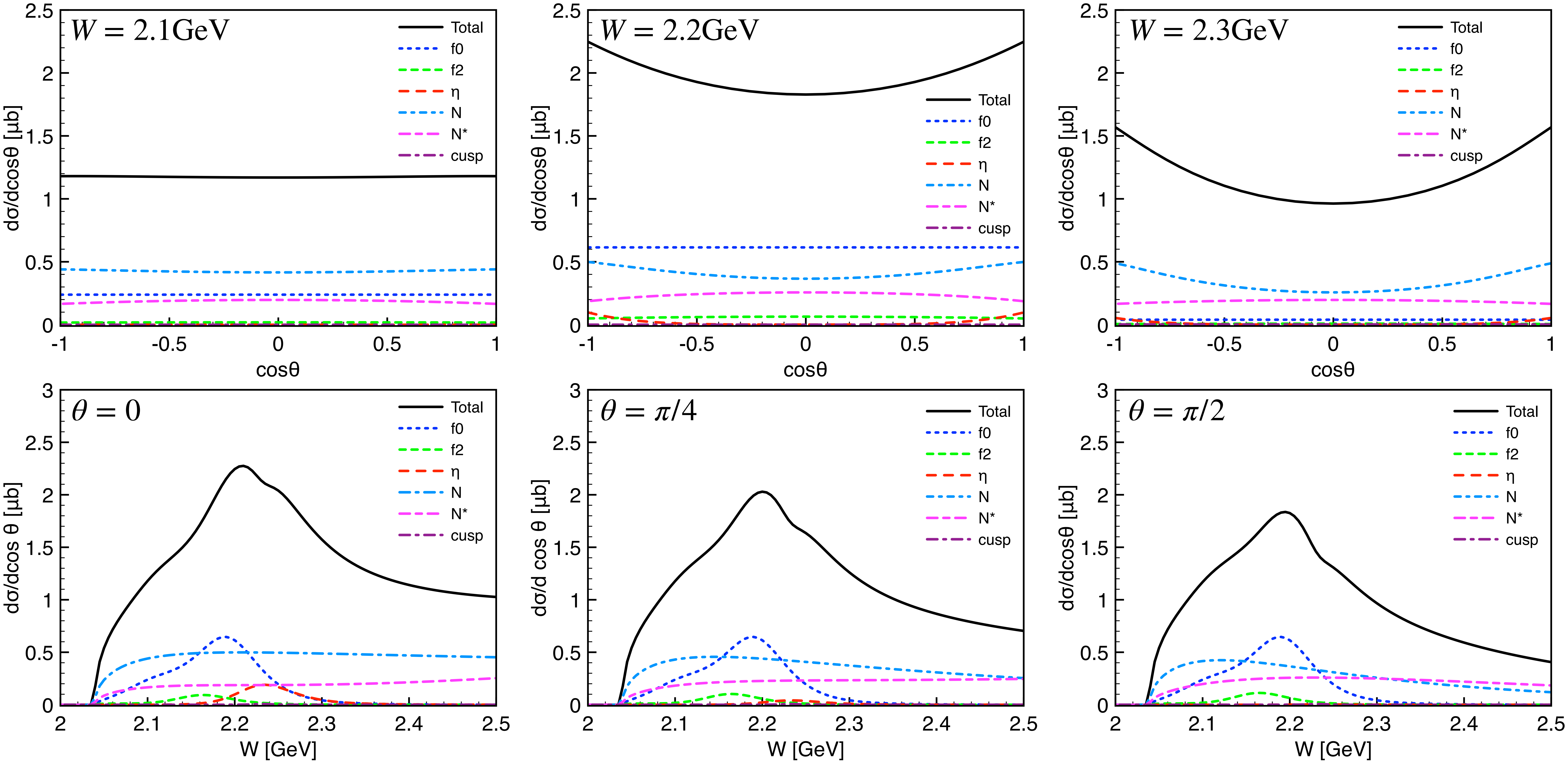

III. Numerical results - $d\sigma/dt$

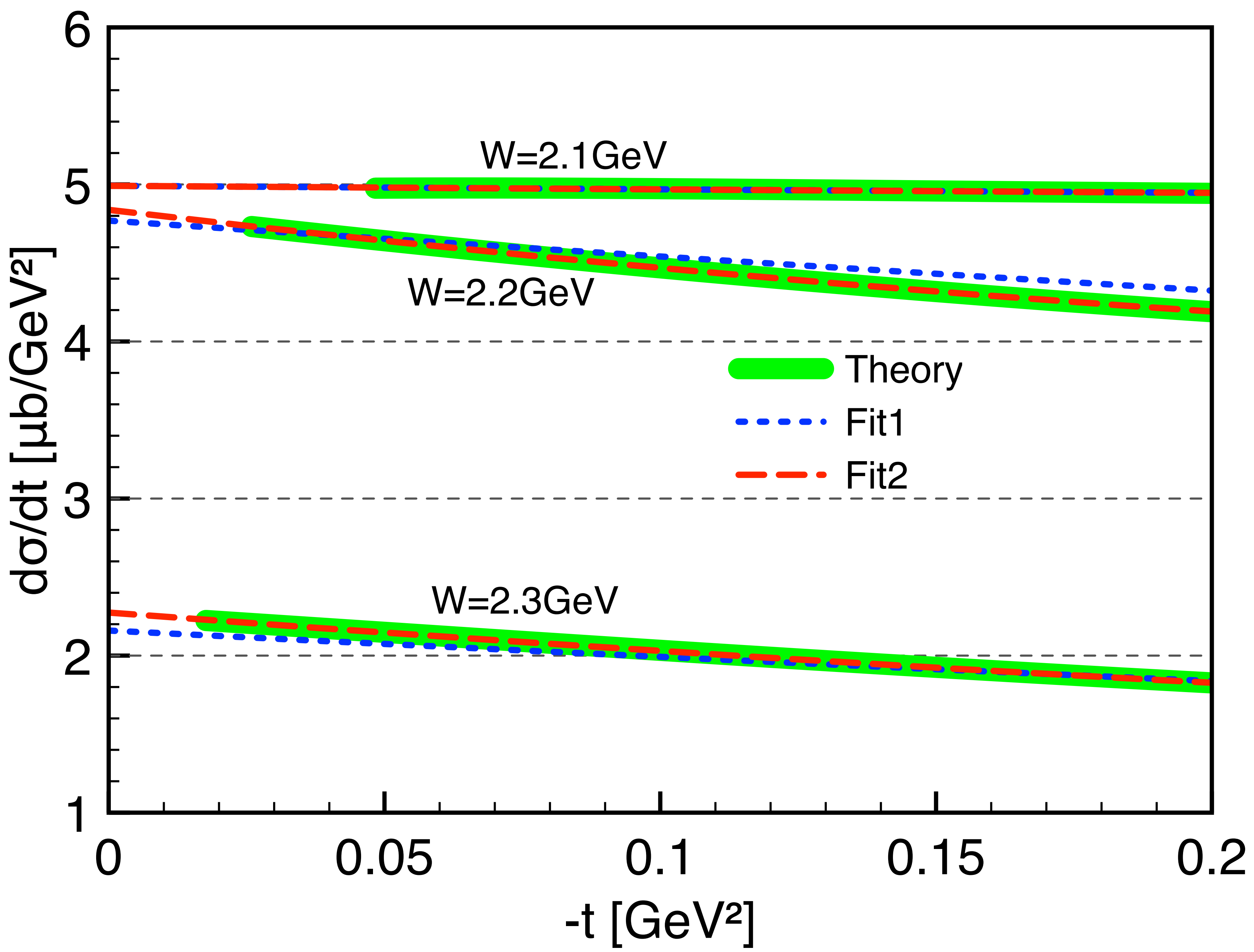

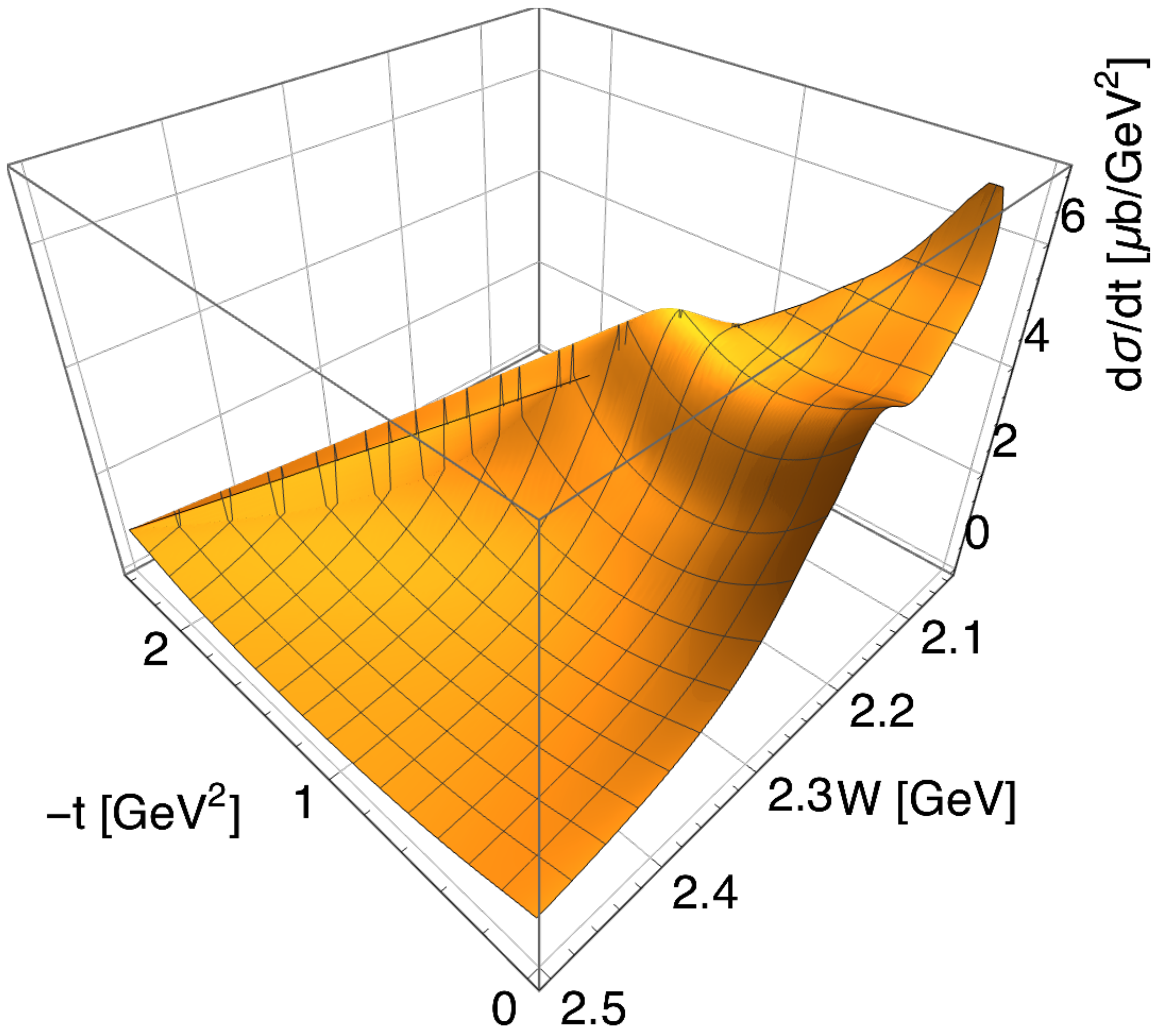

$$\text{Fit1} = ae^{-b|t|}$$

$$\text{Fit2} = a'e^{-b'|t|} + c'e^{-d'|t|}$$

W [GeV]	a	b	a'	b'	c'	d'
2.1	4.99	0.05	3.99	0.05	1.00	0.05
2.2	4.72	0.50	3.80	1.47	1.04	−1.33
2.3	2.21	0.82	2.15	1.36	0.12	−2.10

- The curve shapes change concavely due to the N contribution as W increase.
- To make the current numerical results more accessible, we fit the curves in the region below $|t| < 0.2\text{GeV}^2$.

III. Numerical results - Spin-Density Matrix Element (SDME)

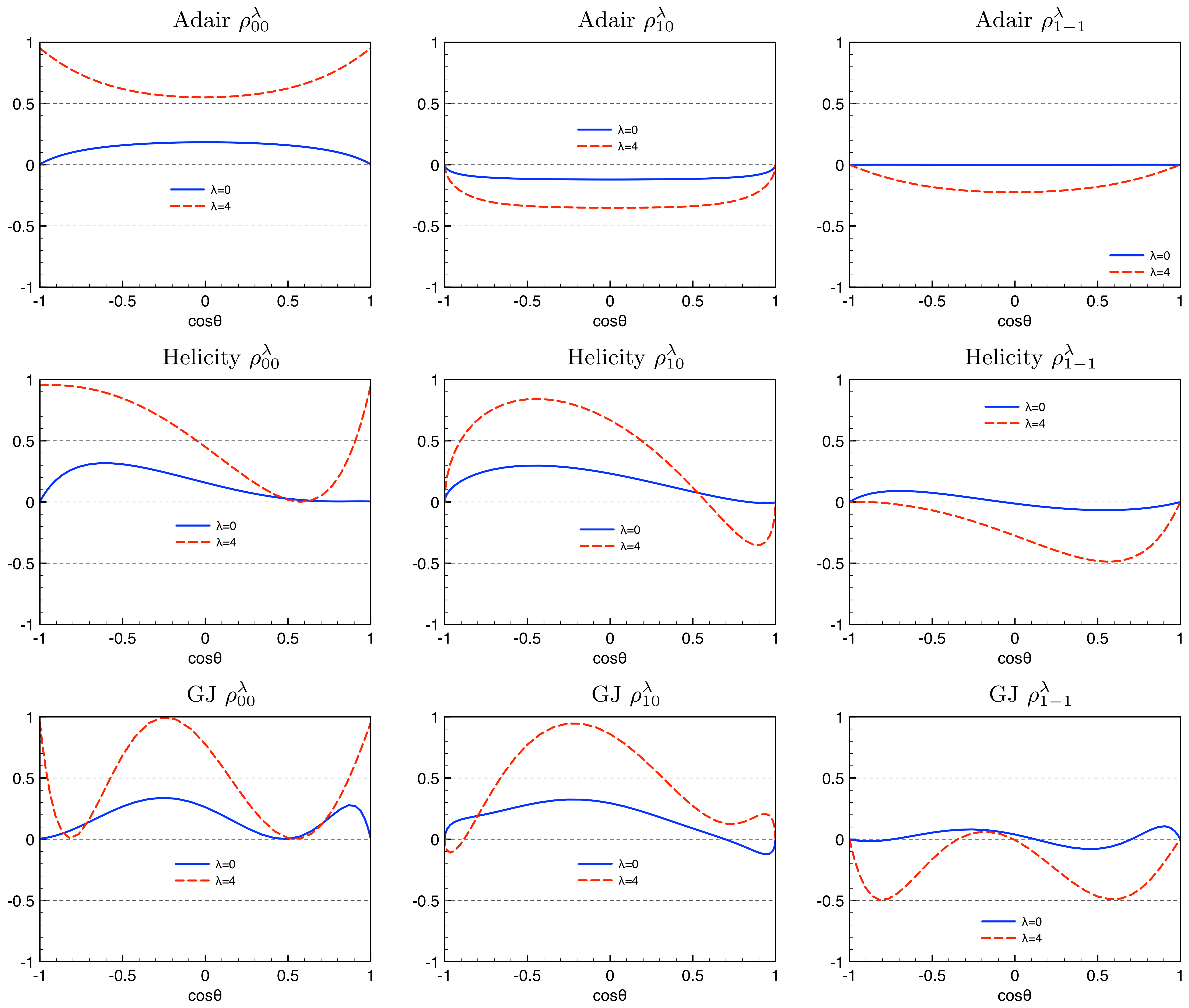

- Each SDME approximately follows specific helicity-flip patterns.

$$\Delta\lambda_{34} = |\lambda_3 - \lambda_4|,\ 0 \leq \Delta\lambda_{34} \leq 2$$

$$\rho^0_{00} \propto |\mathcal{M}_{01}|^2 + |\mathcal{M}_{0-1}|^2,$$
$$\rho^4_{00} \propto |\mathcal{M}_{00}|^2,$$

$$\rho^0_{10} \propto \left(\mathcal{M}_{11}\mathcal{M}^*_{01} + \mathcal{M}_{1-1}\mathcal{M}^*_{0-1}\right),$$
$$\rho^4_{10} \propto \mathcal{M}_{10}\mathcal{M}^*_{00},$$

$$\rho^0_{1-1} \propto \left(\mathcal{M}_{11}\mathcal{M}^*_{-11} + \mathcal{M}_{1-1}\mathcal{M}^*_{-1-1}\right),$$
$$\rho^4_{1-1} \propto \mathcal{M}_{10}\mathcal{M}^*_{-10},$$

- The particles produced in the reaction determine this spin difference, which helps in understanding the particles reaction mechanism.

III. Numerical results - Spin-Density Matrix Element (SDME)

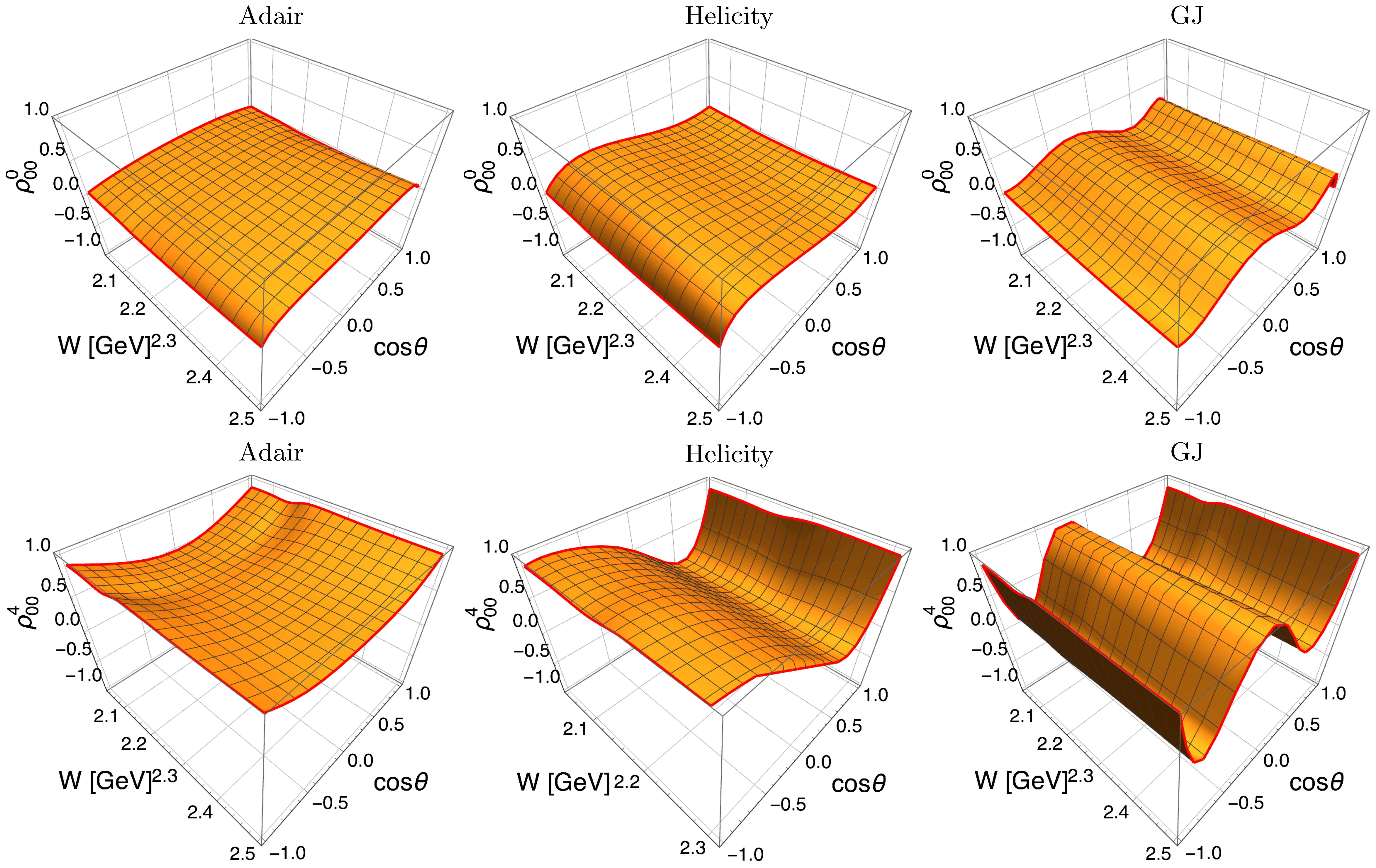

III. Numerical results - Polarization

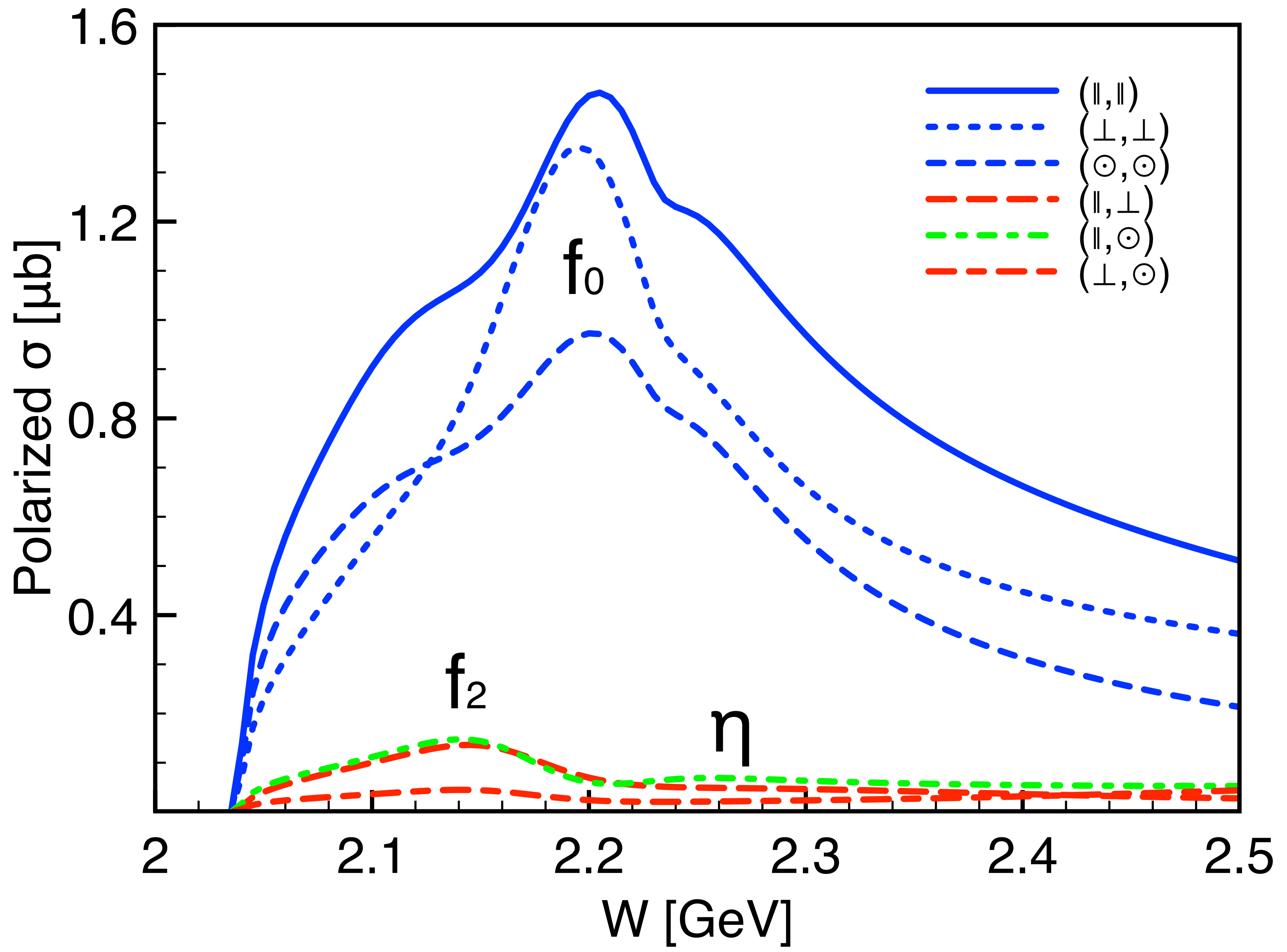

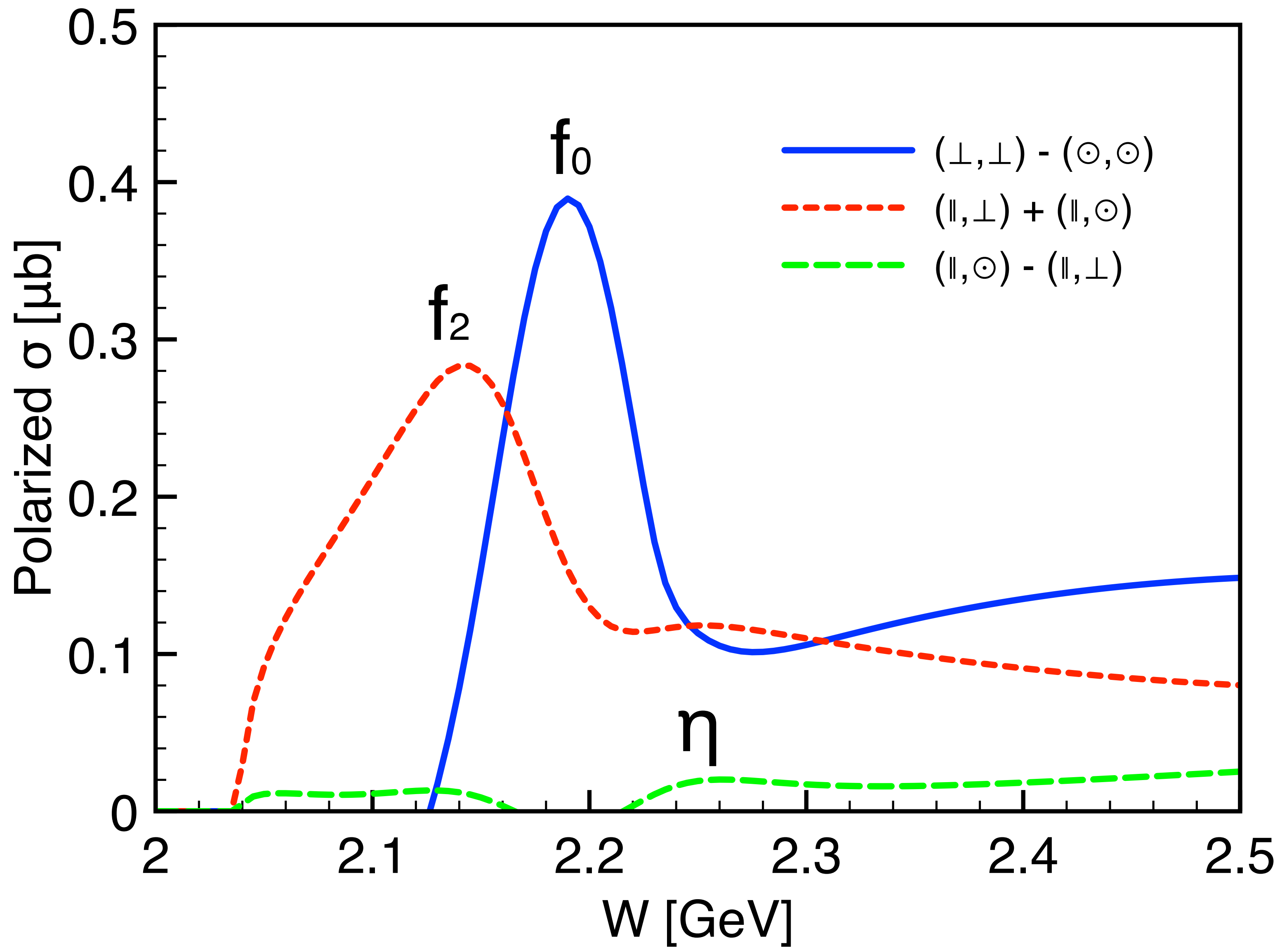

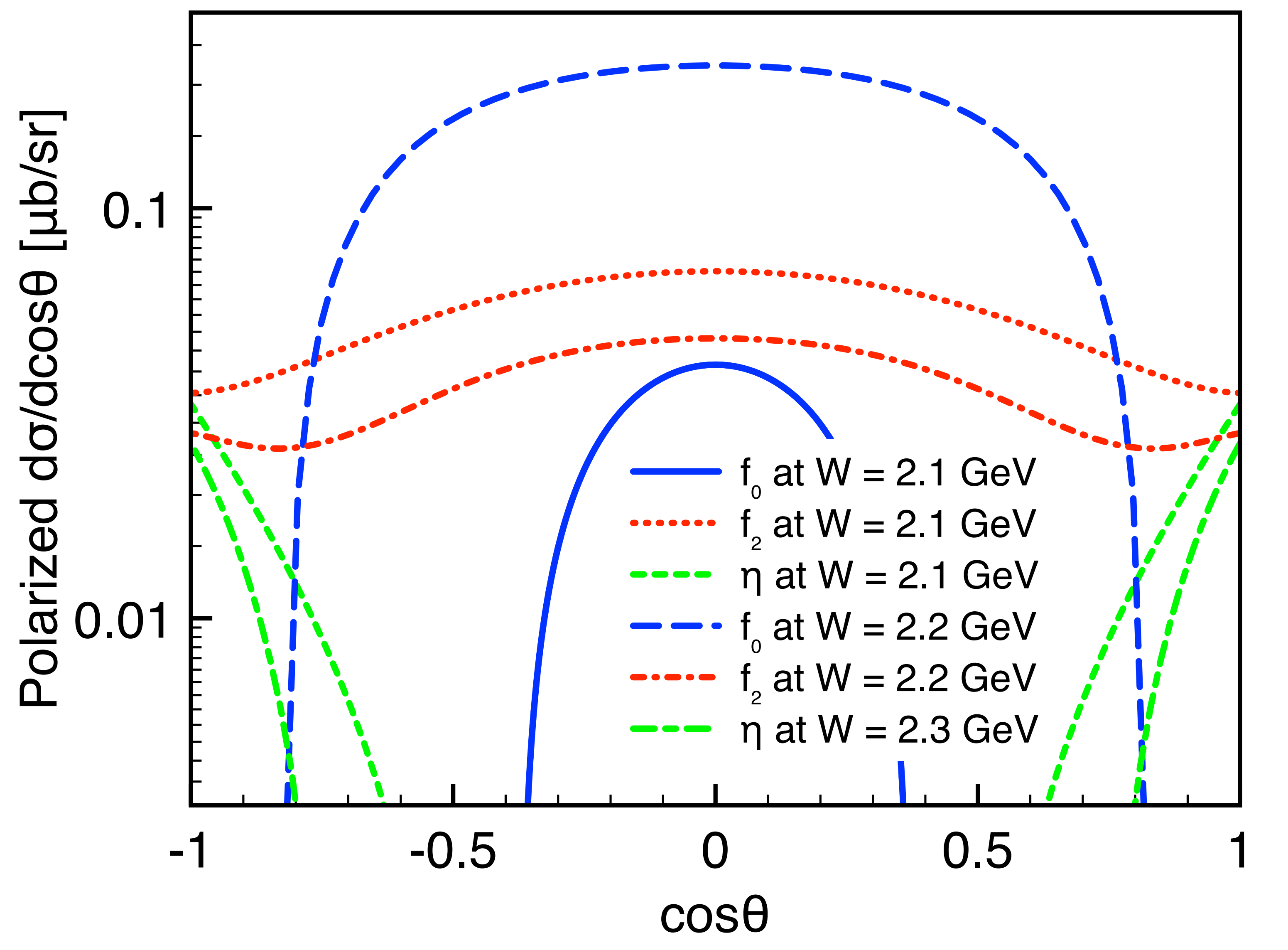

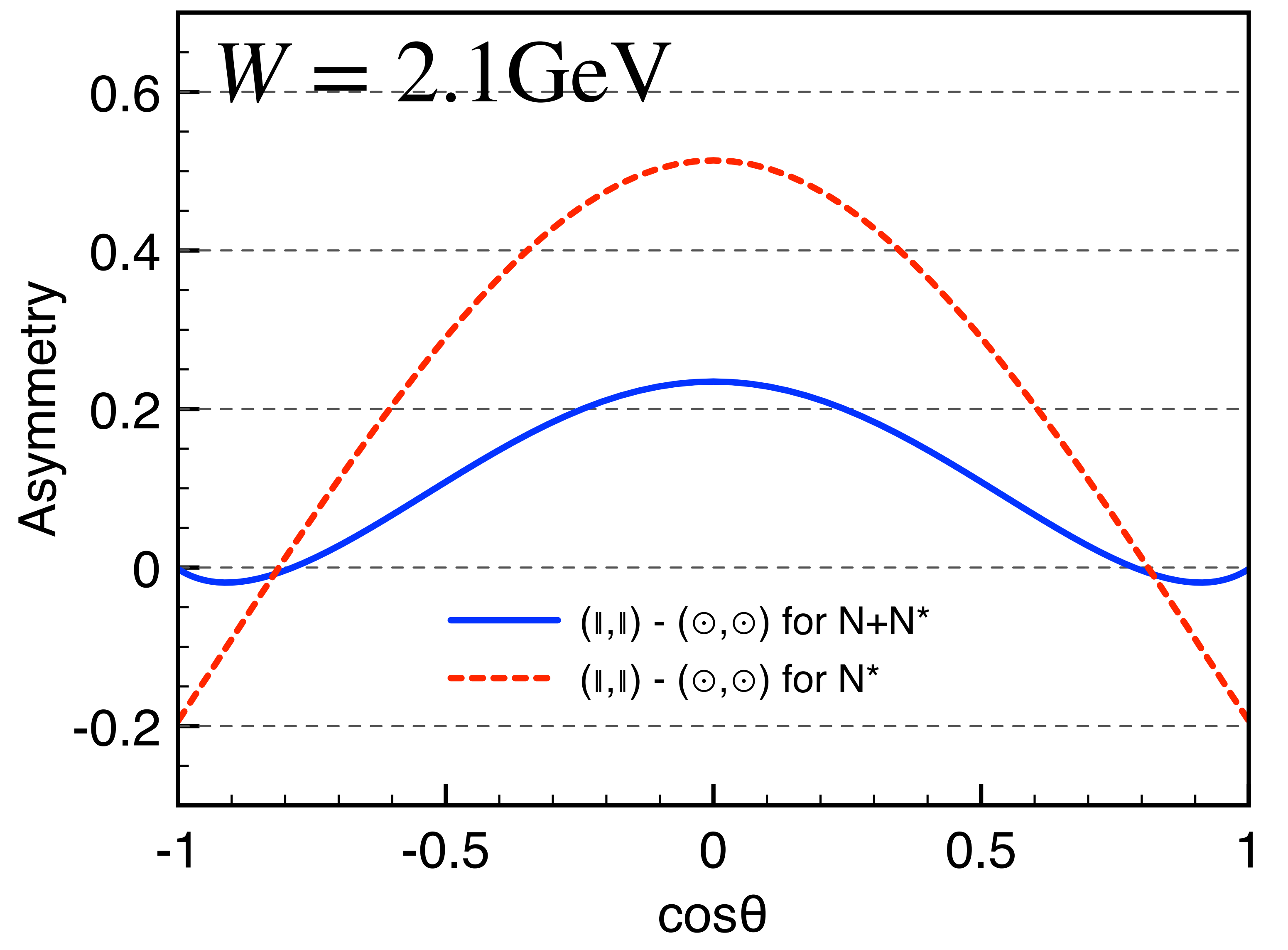

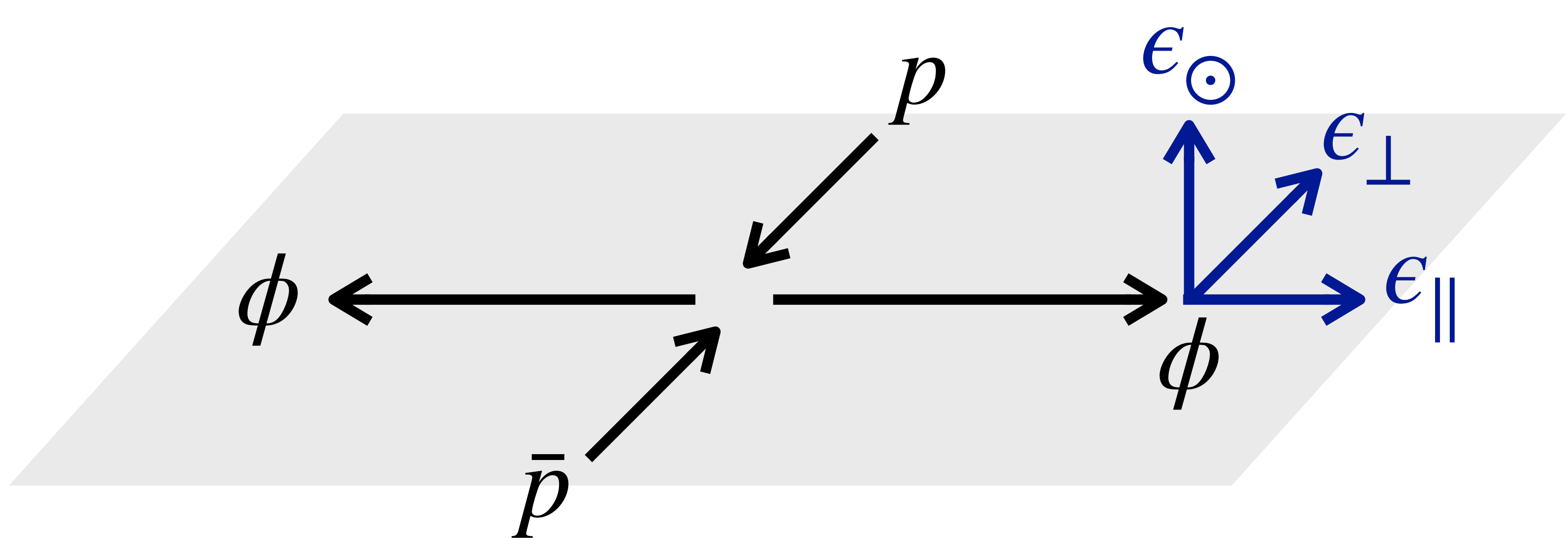

- Amplitudes are sensitive to polarization and are reduced by certain combinations.

$$\text{Asymmetry} \equiv \frac{d\sigma_{\epsilon_3 \epsilon_4} - d\sigma_{\epsilon_3' \epsilon_4'}}{d\sigma_{\epsilon_3 \epsilon_4} + d\sigma_{\epsilon_3' \epsilon_4'}}$$

- By measuring asymmetries, the contribution of N and N* can be determined.

Scattering length in $\pi^- p \to \phi n$ reaction

I. Introduction & II. Theoretical framework

- Studying ϕN interaction characteristics through scattering length.
- A channel to explore N resonances
- Calculating the interaction strength and characteristics of the P_s exotic state.

Feynman diagram and Effective Lagrangian

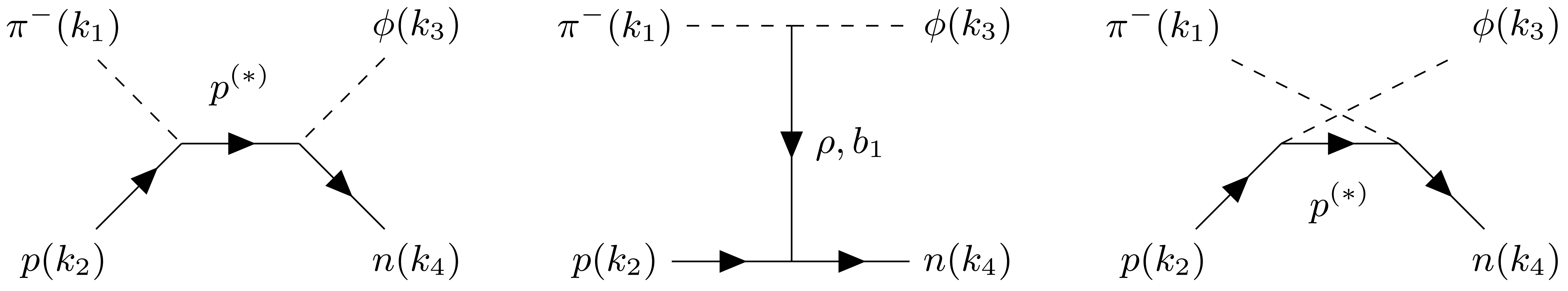

(a) s channel (b) t channel (c) u channel

$$
\begin{aligned}
\mathcal{L}_{PNB_{1\pm}} &= ig_{PNB_{1\pm}}\bar{N}P\Gamma^{\pm}\gamma_5 B_{1\pm} + \text{h.c.},\\
\mathcal{L}_{VNB_{1\pm}} &= g_{VNB_{1\pm}}\bar{N}\Gamma^{\pm}V_\mu\gamma^\mu B_{1\pm} + \text{h.c.},\\
\mathcal{L}_{PNB_{3\pm}} &= \frac{g_{PNB_{3\pm}}}{M_{P_s}}\bar{N}(\partial_\mu P)\Gamma^{\pm}B^{\mu}_{3\pm} + \text{h.c.},\\
\mathcal{L}_{VNB_{3\pm}} &= \frac{ig_{VNB_{3\pm}}}{M_{P_s}}\bar{N}\gamma_5\Gamma^{\pm}F_{V\mu\nu}\gamma^\nu B^{\mu}_{3\pm} + \text{h.c.},\\
\mathcal{L}_{VBB} &= g_{VBB}\bar{B}\gamma^\mu\gamma_5 V^{\dagger}_{\mu}B + \text{h.c.},\\
\mathcal{L}_{VVP} &= \frac{g_{VVP}}{M_P}\epsilon^{\mu\nu\sigma\rho}F^{\mu\nu}_{V}F^{\sigma\rho}_{V}P + \text{h.c.},\\
\mathcal{L}_{ABB} &= g_{ABB}\bar{B}\gamma^\mu A^{\dagger}_{\mu}B + \text{h.c.},\\
\mathcal{L}_{AVP} &= \frac{b}{2\sqrt{2}}\cdot A^{+}_{1\mu}(\sqrt{2}V^\mu P^-)
\end{aligned}
$$

Scattering length

Scattering amplitude $$f(E) = -\frac{\mu}{2\pi}t(E) = \frac{1}{-\frac{2\pi}{\mu v} + \frac{\Lambda^3}{2}\frac{1}{(k+i\Lambda)^2}} = \frac{1}{-\left(\frac{2\pi}{\mu v} + \frac{\Lambda}{2}\right) - ik + \frac{3}{2\Lambda}k^2} = \frac{1}{-\frac{1}{a} - ik + \frac{b}{2}k^2 + \cdots}$$

Scattering length, effective range $$a = \left(\frac{2\pi}{\mu v} + \frac{\Lambda}{2}\right)^{-1}, \quad b = \frac{3}{\Lambda}$$

III. Numerical results

Total Cross Section

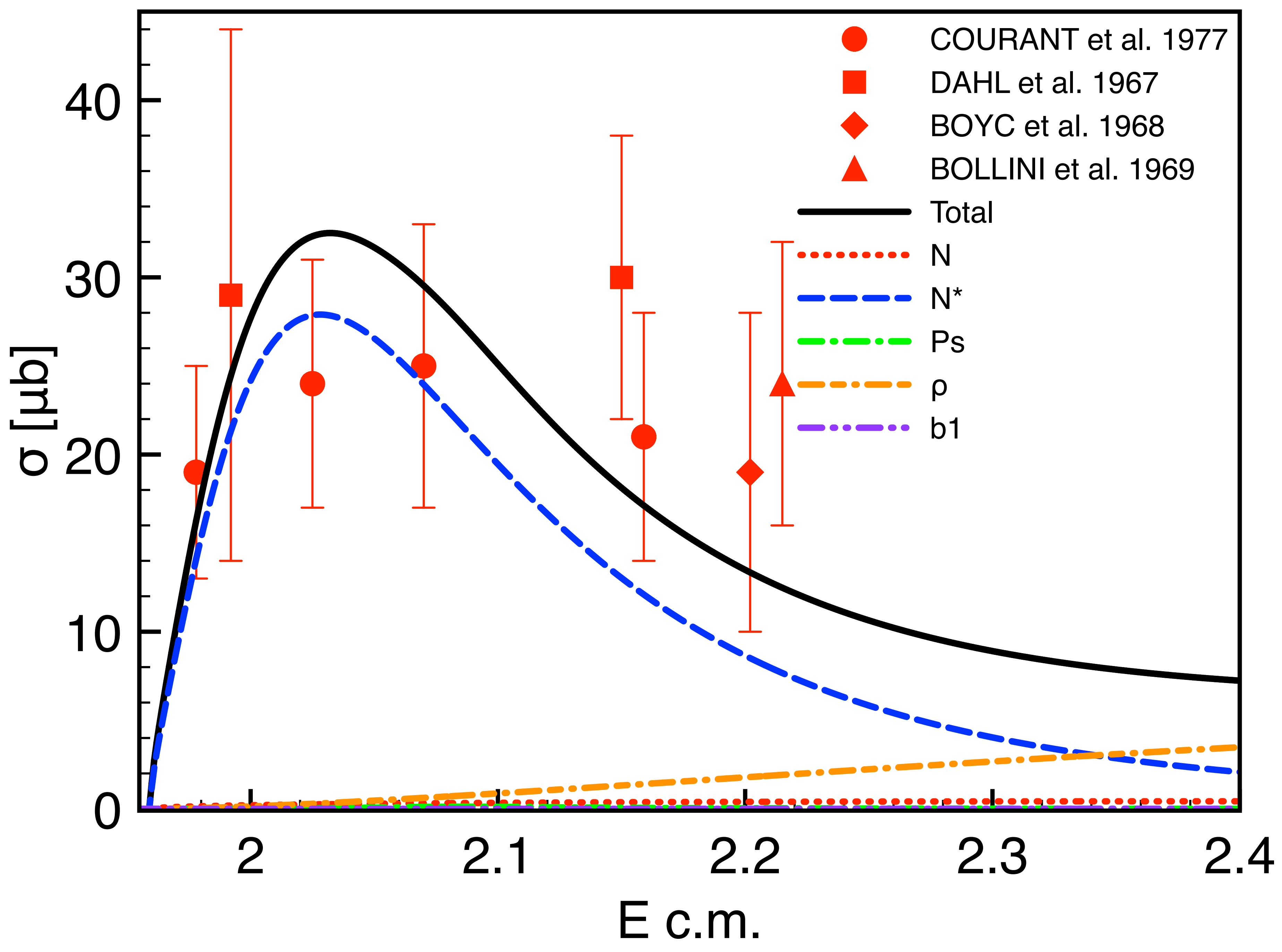

Differential Cross Section

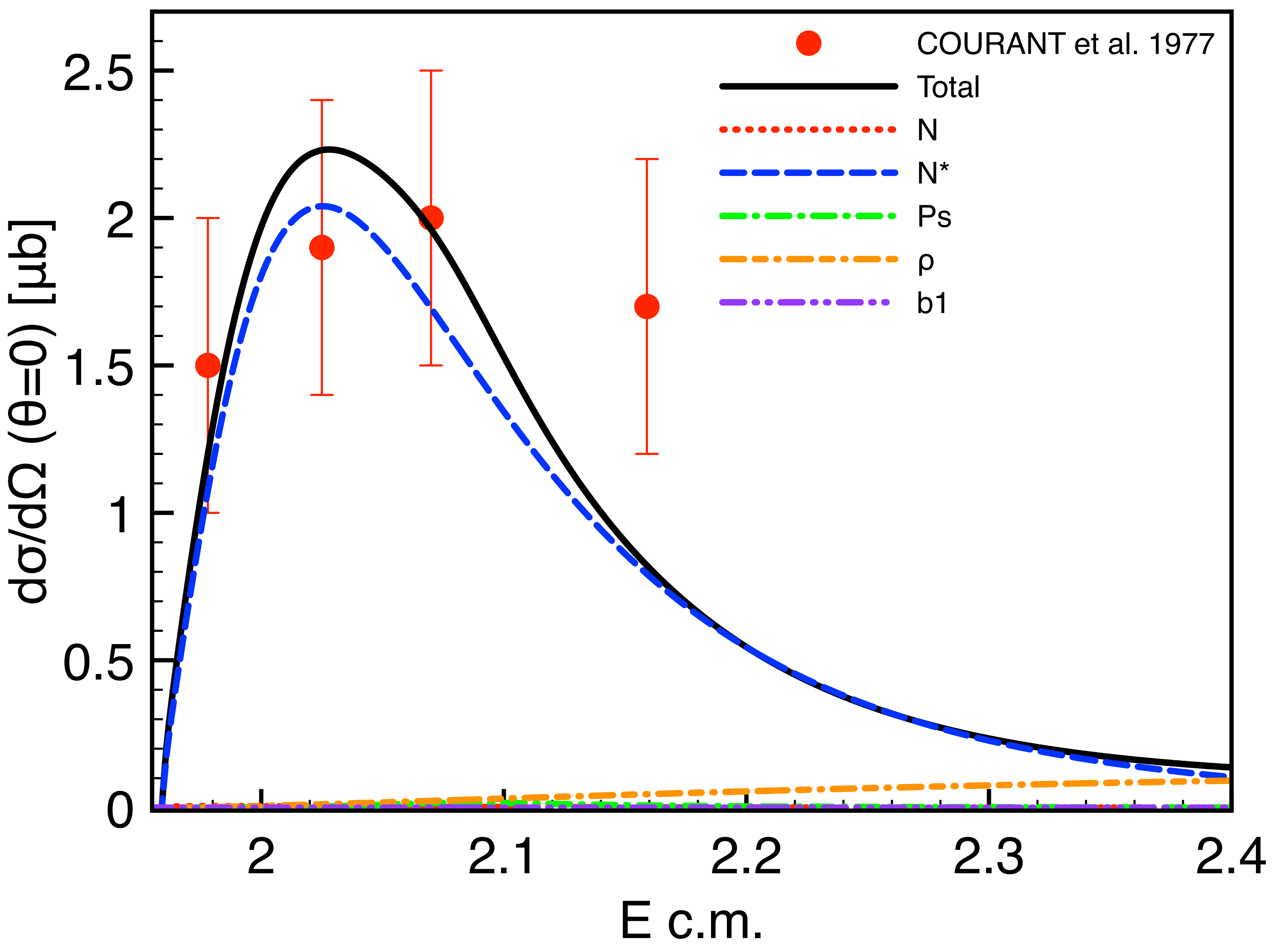

Coupling constants

	N	$N^*(1535,1/2^-)$	$N^*(1650,1/2^-)$		$N^*(1895,1/2^-)$		$P_s(2071,3/2^-)$
$M-i\Gamma/2$ [MeV]	$938-i0$	$1504-i55$	$1668-i28$	$1673-i67$	$1801-i96$	$1912-i54$	$2071-i50$
$g_{\phi NN^{(*)}}$	-1.47	$1.4+i2.2$	$4.1-i2.7$	$4.5+i5.2$	$2.1+i1.8$	$0.9-i0.2$	$0.285+i0.01$
$g_{\pi NN^{(*)}}$	0.989	$0.9-i0.3$	$-0.5-i0.5$	$1.3-i0.6$	$0.5+i0.3$	$0.1-i0.5$	0.330

	$\rho(770)$	$b_1(1235)$
$M-i\Gamma/2$ [MeV]	$763-i73$	$1229.5-i71$
$g_{\phi\pi}$	0.000174MeV^{-1}	2.0MeV
g_{NN}	3.363	8.83

R. L. Workman *et al*, [Particle Data Group], PTEP **2022**, 083C01 (2022)
K. P. Khemchandani *et al*, Phys. Rev. D **88**, 114016 (2013)
X. Y. Wang *et al*, Phys. Rev. D **100**, 014026 (2024)
B. Agatão et al, (unpublished)

IV. Summary

$\bar{p}p \to \phi\phi$

- The total cross section of $\bar{p}p \to \phi\phi$ reactions can be described in terms of the meson pole and baryon exchange diagrams.
- The nontrivial structure around $W = 2.25\mathrm{GeV}$ is well reproduced by the interference between the cusp effect form the $\bar{\Lambda}\Lambda$-loop contribution and other.
- $d\sigma/dt$ was fitted using an single and double exponential function to make the current numerical results more accessible.
- SDME provide crucial information about the reaction mechanism and can serve as benchmarks for future experiments.
- By analyzing the angular distributions of specific polarization combinations, it is possible to determine the contributions of mesons and baryons.
- To validating the theoretical predictions presented in this study, the experiment will be conducted at J-PARC.

$\pi^- p \to \phi n$

- Scattering length will be calculated to investigate the characteristics of the interaction.
- Total cross section and differential cross section are being calculated based on the experimental data.
- Scattering length will be calculated in the future.

Thank you